Original Article
Yonsei Med J 2019 May;60(5):429-439
https://doi.org/10.3349/ymj.2019.60.5.429
Yonsei Medical Journal
YMJ
pISSN: 0513-5796 · eISSN: 1976-2437

Biodegradable Magnesium Alloy Stents as a Treatment for Vein Graft Restenosis

Yugang Li[1], Lei Wang[1], Shanshan Chen[2], Dan Yu[1], Weifeng Sun[1], and Shijie Xin[1]

[1]Department of Vascular and Thyroid Surgery, The First Affiliated Hospital, China Medical University, Shenyang; [2]Institute of Metal Research, Chines Academy of Sciences, Shenyang, China.

Purpose: To explore the effects of biodegradable magnesium alloy stents (BMAS) on remodeling of vein graft (VG) anastomotic restenosis.

Materials and Methods: To establish a VG restenosis model, seventy two New Zealand rabbits were randomly divided into three groups according to whether a stent was implanted in the graft vein or not. BMASs and 316L stainless steel stents were implanted in BMAS and 316L groups, respectively, while no stent was implanted in the no-treatment control group (NC group). Loss of lumen diameter in the graft vein was measured in all three groups. Upon harvesting VG segments to evaluate intimal proliferation and re-endothelization, the degradation and biological safety of the stents were observed to explore the effects of BMAS on VG remodeling.

Results: Model establishment and stent implantation were successful. The BMAS reduced lumen loss, compared with the control group (0.05±0.34 mm vs. 0.90±0.39 mm, p=0.001), in the early stage. The neointimal area was smaller in the BMAS group than the 316L group after 4 months (4.96±0.66 mm^2 vs. 6.80±0.69 mm^2, p=0.017). Re-endothelialization in the BMAS group was better than that in the 316L group (p=0.001). Within 4 months, the BMAS had degraded, and the magnesium was converted to phosphorus and calcium. The support force of the BMAS began to reduce at 2–3 months after implantation, without significant toxic effects.

Conclusion: BMAS promotes positive remodeling of VG anastomosis and has advantages over the conventional 316L stents in the treatment of venous diseases.

Key Words: Restenosis, vascular graft, biodegradable, stent, magnesium

INTRODUCTION

Occlusive vascular disease is a leading cause of human death. Although endovascular therapy has developed quickly, autologous vein bypass grafting remains the most effective treatment for occlusive vascular disease, especially in coronary artery disease.[1,2] However, autologous vein bypass grafting has some disadvantages: For instance, 10% to 15% of vein grafts (VGs) are occluded at 1 year after surgery, and half of the grafts lose their function within 10 years[3] due to vein graft failure (VGF), for which VG stenosis is the main cause. Endovascular treatment, including balloon dilation, bare metal stent (BMS), and drug-eluting stent (DES), can effectively improve the prognosis of VGF.[4-7] Nevertheless, endovascular treatment for VGF still has long-term issues, including long-term thrombosis, excessive proliferation of the intima, long-term use of antiplatelet drugs, and other serious adverse events.

The emergence of biodegradable stents has opened new promising avenues for the treatment of VGF. Biodegradable magnesium alloy stents (BMASs) are the most studied biodegradable scaffolds. Compared to an absorbable polymer stent, BMAS has a better bracing force and tissue compatibility. In 2003, magnesium alloy stents composed of the alloy AE21 (containing 2% aluminum and 1% rare earths) were implanted in the coronary arteries of swine for the first time.[8] In 2013, Haude,

Received: January 9, 2019 **Revised:** February 27, 2019
Accepted: March 1, 2019
Corresponding author: Shijie Xin, PhD, Department of Vascular and Thyroid Surgery, The First Affiliated Hospital, China Medical University, Shenyang 110001, China.
Tel: 86-24-8328-3288, Fax: 86-24-8328-3288, E-mail: sjxin@cmu.edu.cn

•The authors have no potential conflicts of interest to disclose.

et al.[9] reported the results of the first drug-eluting absorbable metal scaffold (DREAMS). In the same year, the second-generation drug-eluting absorbable metal scaffold (DREAMS 2G), which had an improved stent structure and used rapamycin as the eluting drug, was also put into a clinical trial. Therein, a loss of lumen diameter of 0.27±0.37 mm and a target vessel failure rate of 3% at 6-month follow-up were reported.[10]

Initially validated for the treatment of coronary artery disease, BMASs have not yet been analyzed for the treatment of VGF. In the present study, we implanted a BMAS into a VG anastomotic stenosis animal model to investigate the stent degradation process and its influence on VG remodeling. The results of this study were expected to provide new evidence for the potential clinical application of BMASs for the treatment of VGF.

MATERIALS AND METHODS

Animals and experimental design

In total, seventy two New Zealand white rabbits, weighing 2.5± 0.2 kg, were provided standard food and care. Autologous jugular-abdominal aorta transplantation was performed on the experimental animals (Fig. 1A). Then, the animals were randomly divided into one of the following three groups at 1 month after transplantation: no-treatment control (NC) group (n=24), 316L group (n=24), and BMAS group (n=24). A BMAS was implanted in the graft vein in the BMAS group, and a 316L stainless steel stent was implanted in the 316L group. No stent was implanted in the NC group. The animals in each group were anaesthetized and sacrificed at 1 month (n=6), 2 months (n=6), 3 months (n=6), and 4 months (n=6) after stent implantation to obtain specimens. Histological experiments were performed on the specimens of the grafted veins and internal organs. Blood samples were collected before the animals were sacrificed.

The BMAS and 316L stainless steel stent used in the experiment were both provided by the Institute of Metal Research, Chinese Academy of Sciences (Shenyang, China). The BMAS was a balloon-expandable stent and laser cut from a AZ31B magnesium alloy tube with a 3-mm diameter and 15-mm length and with a stent strut diameter of 155±65 mm (Fig. 1B). 316L stainless steel stents with the same specifications were used as controls. The surface of the BMAS was treated with a chemical conversion coating and a polymer coating to effectively control the degradation rate. The radial support force could reach 10.9 N when the BMAS was extended to 3 mm (Fig. 1C).

All procedures obeyed the animal study ethics authorized by the Animal Care Committee of Chinese Medical University. We also obtained IACUC approval (No. 201603027).

Animal model and stent implantation

To perform autologous jugular-abdominal aorta transplantation, animals were anesthetized with an intravenous injection of 30 mg/kg of phenobarbital. All surgical procedures were performed under sterile conditions. The left external jugular vein, with a length of 0.8 cm, was end-to-end grafted onto the infrarenal abdominal aorta using 9/0 vascular sutures (Ethicon, Inc., Shanghai, China) in a nonreversed configuration (Fig. 1D). Twelve interrupted sutures were required to seal each end. The infrarenal abdominal aorta was clamped for an average of 45 min. The incision was disinfected thoroughly with penicillin saline and sutured layer by layer. Penicillin was given for 3 days in a row after the operation to prevent postoperative infection.

Animals were anesthetized again at postoperative 1 month. Digital subtraction angiography (DSA) was carried out via the marginal ear vein to measure the diameter of the abdominal aorta, as well as proximal and distal anastomosis of the VG. Two stents were randomly selected for implantation into the narrow anastomosis of the VG. Animals without stent implantation were used as NCs. Therein, a surgical incision was made in the neck, and the right carotid artery was exposed. A 5-F micropuncture set (Cook Inc., Bloomington, IN, USA) was inserted into the common carotid artery. A 4-F pigtail catheter (Terumo Medical Corporation, Somerset, NJ, USA) was transported to the infrarenal abdominal aorta to obtain high-resolution abdominal aortic artery angiography and to determine the VG position and length. Heparin (200 U/kg) was instilled through the catheter to prevent thrombosis before stent implantation. The BMAS and the 316L stents with a balloon were delivered to the VG across the anastomosis at both ends. The balloon was dilated by inflation at 6 atm of pressure for 30 s, which was repeated three times. After the stent was released, abdominal aortic angiography was used to confirm that the anastomotic stenosis of the grafted vein was patent and supported by the stent. The right carotid artery was ligated, and the incision was sutured layer by layer. All animals were treated with oral aspirin (2 mg/kg/d) until sacrificed to prevent thrombosis.

Follow-up observation

DSA and ultrasonography were carried out at different time points after stent implantation under anesthesia. 10 mL of iohexol was injected into the auricular vein to obtain the VG segment images. The diameter of the two-end anastomosis was measured by DSA. Diameter loss of anastomosis is defined as the difference between abdominal aortic diameter and anastomotic diameter. Doppler ultrasonography was performed sequentially to observe the morphology of the stent and VG anastomosis.

Histology

Animals were sacrificed at the 1, 2, 3, and 4 months after implantation to obtain the VG specimens. Ligation of the infrarenal abdominal aorta and the bilateral iliac artery was performed in the animals (n=3 per group) that were used to observe neointimal proliferation. An incision in the unilateral internal iliac artery was made, and VG was irrigated with heparinized saline

https://doi.org/10.3349/ymj.2019.60.5.429

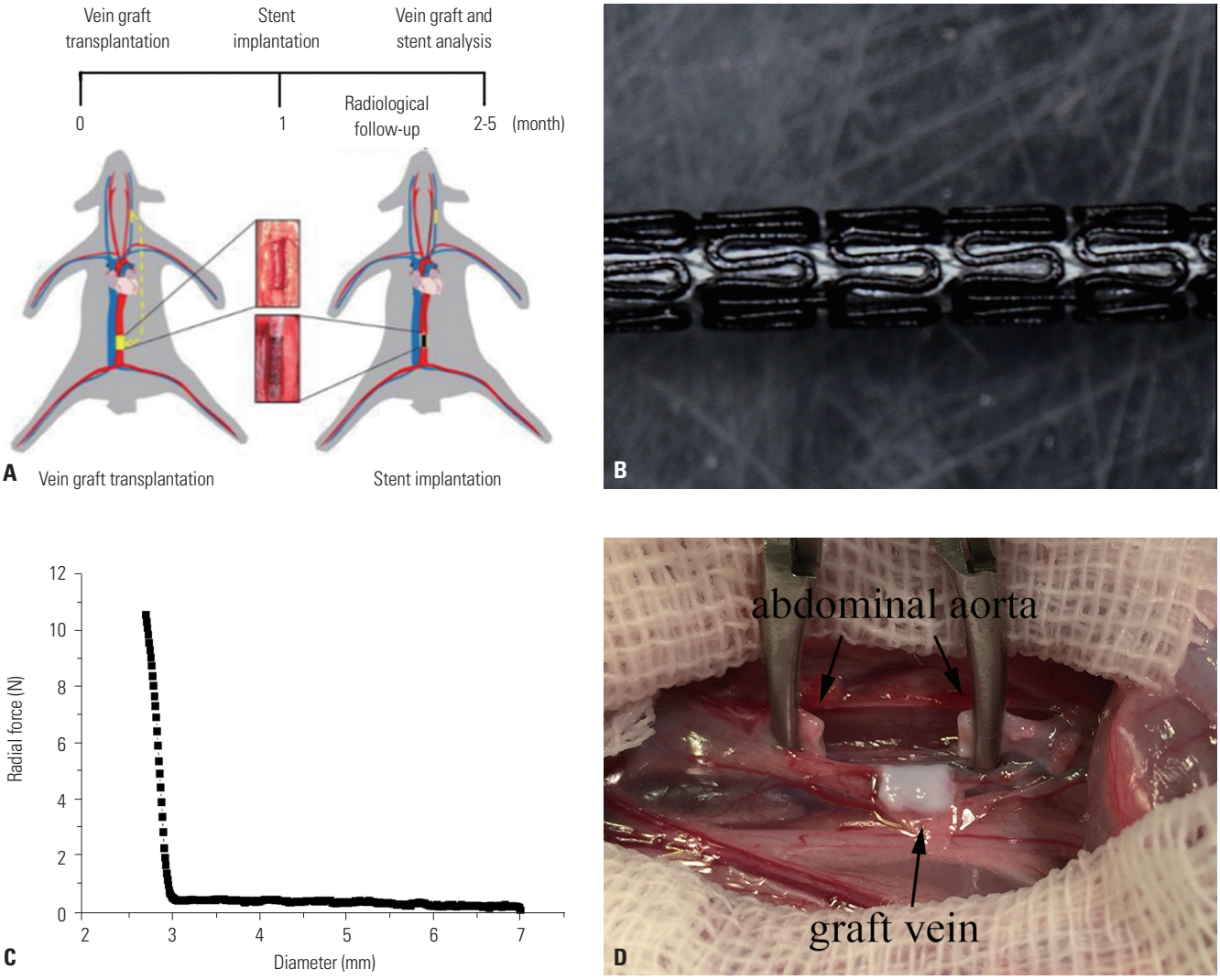

Fig. 1. Stent design and vein graft model. (A) Study design. (B) Demonstration of BMAS. (C) BMAS support force test. (D) Surgery of vein transplantation. BMAS, biodegradable magnesium alloy stents.

three times (10 mL per time) through the catheter-punctured abdominal aorta. Thereafter, polyformaldehyde was infused for 30 min with a pressure of 100 mm Hg. The VG specimens were excised at both ends of the anastomosis at a 2-mm distance from the suture. Stents in the sample were dissolved in 10% nitric acid for 20 min. The VG specimens were fixed in formalin and xylene and dehydrated in graded ethanol, followed by paraffin embedding or neutral resin packaging. Hematoxylin and eosin (H&E) and elastic Verhoeff-van Gieson staining were performed according to standard protocols. The staining was observed under an ordinary optical microscope (TE2000-S, Nikon, Tokyo, Japan). ImageJ 1.41 software (National Institutes of Health, Bethesda, MD, USA) was used to measure the internal elastic lamina (IEL) and lumen area. Neointimal area was defined as the difference between IEL and lumen area.

Evans blue

Animals (n=3) were injected with 0.5 mL/kg of 0.5% Evans blue solution at 30 min before sacrifice: Evans blue dye can dye vascular intima not covered by endothelial cells. The anastomotic specimens were put into 1 mL of formamide solution at 4°C overnight to extract the dye. After extraction, 100 μL of formamide was placed in a 96-well plate, which was measured at a wavelength of 620 nm using a spectrophotometer (Model 680, Bio-Rad, Hercules, CA, USA).

Determination of scaffold degradation

The anastomotic specimens were fixed with 2.5% glutaraldehyde solution. Specimens were cut along the vascular axis and then fixed on a filter paper. After the sample was dehydrated, dried, and treated with an alcohol gradient, the blood vessel endothelium was examined. To observe the degradation products of the scaffold, specimens were dehydrated in increasing alcohol concentrations and vertically embedded in epoxy resin, followed by cross-section preparation. Thereafter, scanning electron microscopy (SEM) and X-ray energy dispersive spec-

trometry (EX250, HORIBA Scientific, Kyoto, Japan) were performed to analyze the chemical composition.

X-ray tomography

Parts of the VG samples were examined with high-resolution X-ray tomography (XRT). Briefly, specimens were placed in an Eppendorf tube for XRT (VersaXRM-500, Carl Zeiss, Jena, Germany) examination. The threshold value of the three-dimensional pixel was set to 1 mm. Two-dimensional images were obtained by a direct scan, followed by three-dimensional reconstruction. The optimum threshold was chosen to separate the stent from the vascular tissue background.

Determination of biocompatibility

Blood samples were collected from the auricular median artery at different time points after stent implantation. The serum from each animal was collected to analyze the blood biochemical indices (AU2700, Olympus, Tokyo, Japan), including K, Na, Cl, Ca, P, Mg, glutamic pyruvic transaminase, alkaline phosphatase, total protein, human albumin, total bilirubin, urea, creatinine, and fibrinogen. Internal organ tissues (heart, liver, spleen, lung, and kidney) were simultaneously obtained when the animals were sacrificed, then fixed, paraffin embedded, and sectioned at a 5-μm thickness. Five sections were selected per organ and stained with H&E. The pathological conditions of the specimens were determined by two pathologists who were blinded to the group classifications.

Statistical analysis

All values are expressed as a mean±standard deviation. When equal variance and normality were observed, analysis of variance followed by the least significant difference test or the Student's t test was used to determine the significant differences between groups. When either the equal variance test or normality test failed, the Kruskal-Wallis (with Dunn's method for post hoc) or Mann-Whitney U test was used. p values <0.05 were considered indicative of a statistically significant difference. Analyses were conducted using Statistical Product and Service Solutions software (SPSS Statistics 19.0, IBM Corp., Armonk, NY, USA).

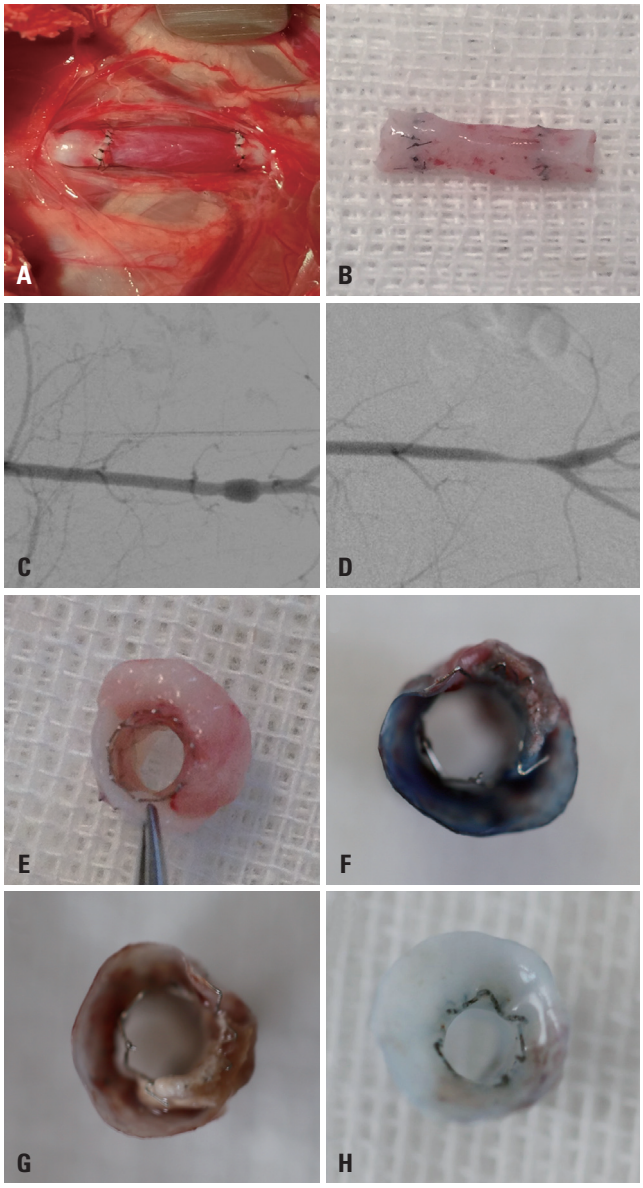

Fig. 2. General information regarding transplantation and implantation during the experimental process. (A and B) The graft vein. (C and D) Digital subtraction angiography examination of the graft vein. The graft vein with stent implanted (C) and graft restenosis (D). (E-G) Formation of atherosclerotic plaque between the stent and vein in three animals of the 316L group. (H) Representative vein graft specimen from the BMAS group. BMAS, biodegradable magnesium alloy stents.

RESULTS

General information regarding transplantation and implantation during the follow-up period

The procedures of vein transplantation and stent implantation were all successful, and all experimental animals survived and were followed up (Fig. 2A and B). No systemic toxicity was observed, and no VG occlusion, stent migration, or thrombosis was observed by ultrasonography during the follow-up period. As examined by DSA, the morphology of the VG and restenosis could be observed (Fig. 2C and D). In the 316L group, three animals were found to have atherosclerotic plaque formation between the stent and the vein; this finding was not identified in the NC or BMAS group (Fig. 2E-H).

Comparison of diameter loss and the neointimal area of the VG between the control, 316L, and BMAS groups

There was no significant difference in the diameter of the anastomosis or the proximal or distal ends among these three groups at 1 month after transplantation. The lumen diameter

https://doi.org/10.3349/ymj.2019.60.5.429

of the anastomosis was obviously improved due to the support of the stent. After stent implantation, the diameter loss of the VG anastomosis was observed by DSA (Fig. 3A). At 1 month after stent implantation, the anastomotic diameter loss at proximal anastomosis in the BMAS (0.05±0.34 mm) and 316L (0.27±0.17 mm) groups was less than that in the NC group (0.90±0.39 mm, p=0.001 and p=0.006, respectively). Results were similar for distal anastomosis (BMAS 0.23±0.26 mm vs. NC 0.85±0.29 mm, p=0.016 and 316L 0.32±0.43 mm vs. NC 0.85±0.29 mm, p=0.028). There were no significant differences between the BMAS and 316L groups. At 2 months, diameter loss at both the proximal and distal anastomoses of the BMAS group was less than that in the NC group. However, diameter loss in the 316L group was greater than that of the BMAS group. Due to BMAS degradation, the radial force began to decrease gradually at 3 months after implantation, while the proximal anastomotic diameter loss of the BMAS group was still less than that of the NC group and the 316L group (BMAS vs. NC, p=0.004, BMAS vs. 316L, p=0.011). There were no significant differences among these groups at 4 months after implantation. Overall, the BMAS significantly improved anastomotic diameter during the early period after implantation, and its support force was comparable to that of the 316L stent (Fig. 3B).

Next, we used ImageJ software to measure the neointimal area of VG among the three groups by elastic Verhoeff-van Gieson staining (Fig. 3C). Neointimal area was defined as the difference between IEL and lumen area. No significant difference in the area of IEL between these groups was observed during the follow-up period. During the follow-up period, the lumen area of the anastomosis decreased gradually, while the neointimal area increased gradually. There were no significant differences in the neointimal areas between these groups at 1 month after stent implantation. However, at 4 months the 316L group significantly increased neointimal areas, compared with the NC group (6.80±0.69 mm^2 vs. 4.12±0.62 mm^2, p=0.005). While the neointimal area in BMAS group was smaller than 316L group at 4 months (4.96±0.66 mm^2 vs. 6.80±0.69 mm^2, p=0.017), and there was no difference between BMAS and NC group (p=0.290) (Fig. 3D).

Next, endothelial repair of the VG was analyzed with Evans blue staining and SEM. Evans blue staining decreased gradually in the BMAS and NC groups, but not in the 316L group. There were no significant differences at the various follow-up time points between the BMAS and NC groups. At 4 months after

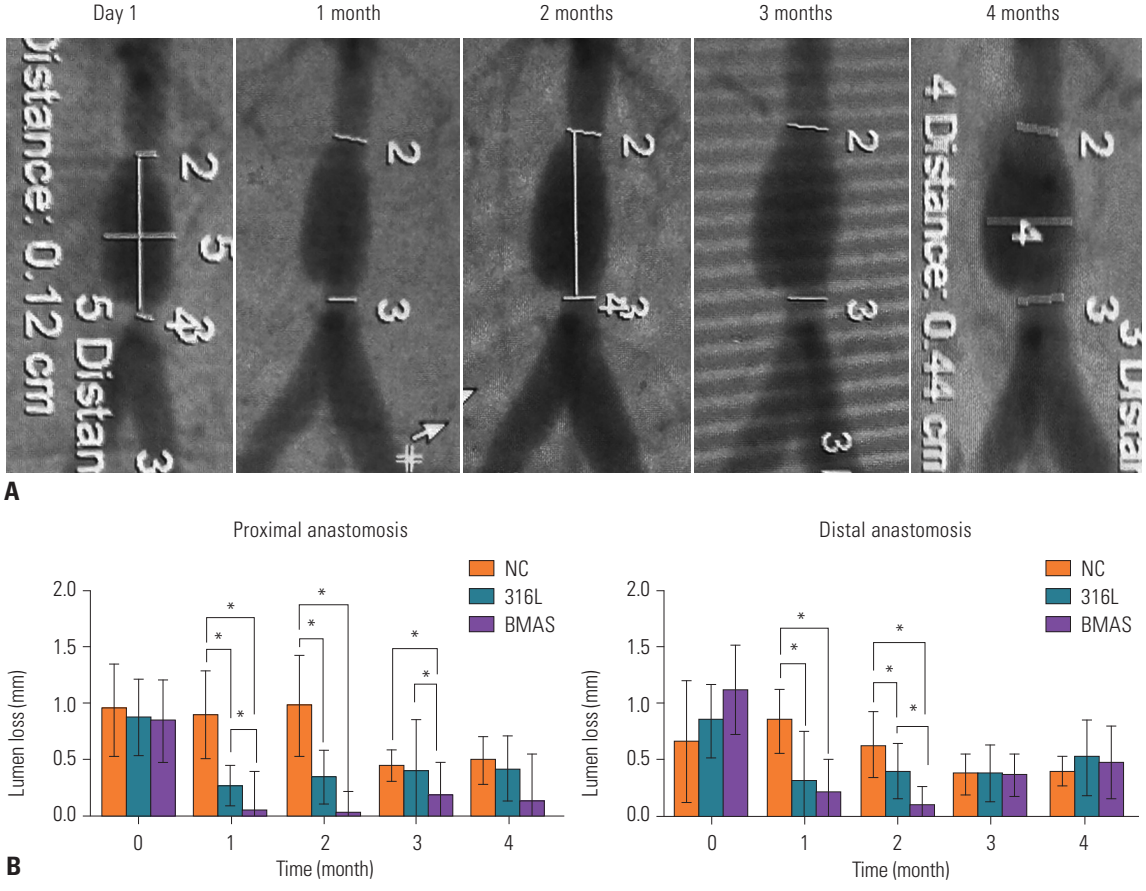

Fig. 3. Comparison of diameter loss and neointimal area of the graft vein between the NC, 316L, and BMAS groups. (A) Demonstration of the measurement of the anastomotic diameter of the graft vein by digital subtraction angiography. (B) Statistical analysis of the lumen diameter loss of the proximal and distal anastomosis of the graft vein between the control, 316L, and BMAS groups.*p<0.05. NC, no-treatment control; 316L, 316L stainless steel stent; BMAS, biodegradable magnesium alloy stent.

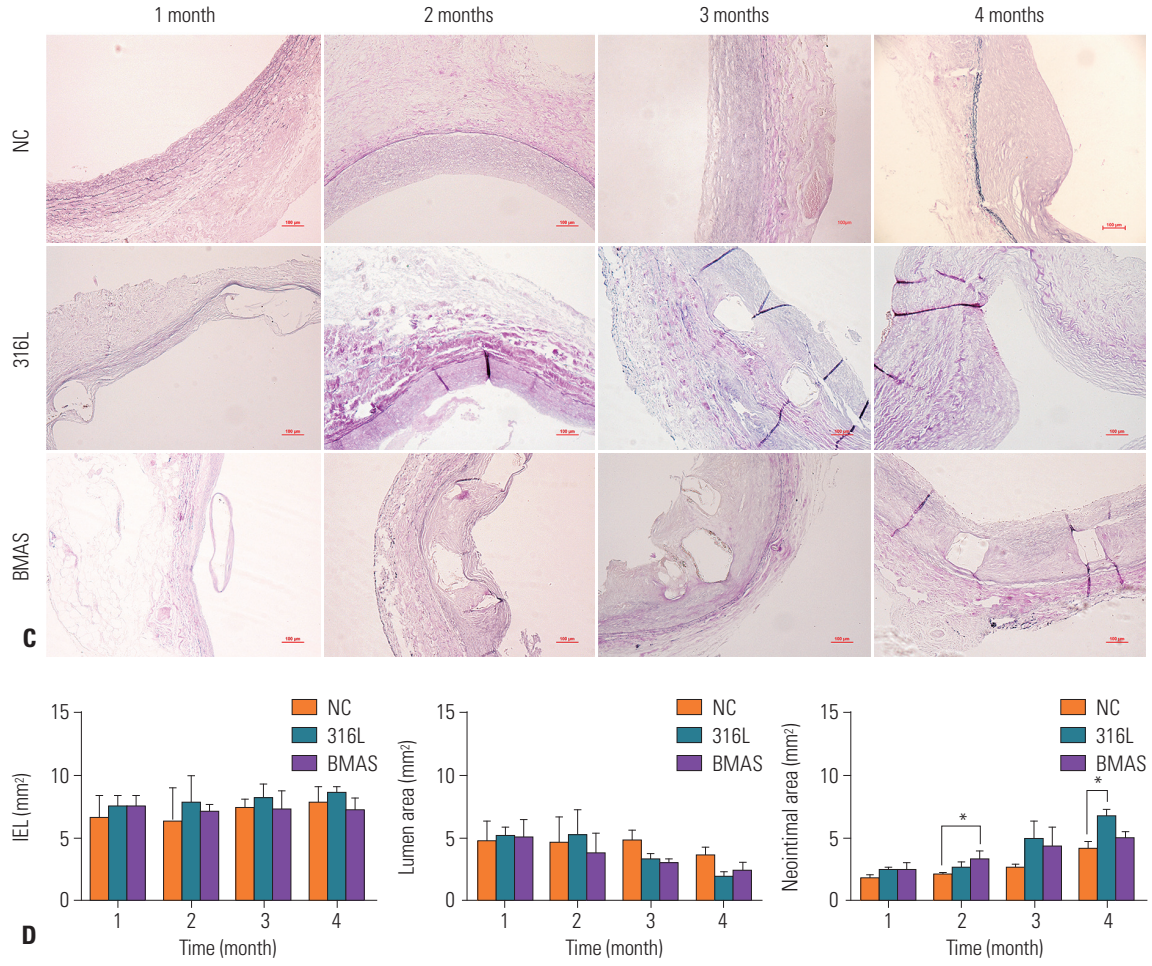

Fig. 3. Comparison of diameter loss and neointimal area of the graft vein between the NC, 316L, and BMAS groups. (C) Elastic Verhoeff-van Gieson staining of the graft vein anastomosis (×100). (D) Statistical analysis of the neointimal area at different follow-up time points as indicated. *p<0.05. NC, no-treatment control; 316L, 316L stainless steel stent; BMAS, biodegradable magnesium alloy stent; IEL, internal elastic lamina.

stent implantation, the OD value of the 316L group was significantly higher than that of the other two groups (0.188±0.320 vs. 0.084±0.010, p=0.001) (Fig. 4A and B), suggesting a decrease in Evans blue staining, which suggests poor endothelial repair. At 2 months after stent implantation, SEM showed that the surface of the stent was covered with smooth muscle cells. A small number of endothelial cells was also observed. At 4 months after implantation, the surface of the BMAS was very smooth and the endothelium of the VG was well repaired. However, the 316L stent wire showed a large number of exposed vascular smooth muscle cells (VSMCs), and the VG re-endothelialization was delayed (Fig. 4C), suggesting that the BMAS promotes re-endothelialization.

BMAS degradation

Next, we examined the degradation of the BMAS with XRT and H&E staining. At 1 month after the BMAS implantation, the scaffold was supported well, and the shape was complete, as revealed by XRT. Within 2–3 months, the continuity of the stent was gradually lost, and the structure of the BMAS was incomplete. Through XRT, we found that the contrast of the bracket had changed, indicating that the metal content had changed. At 4 months, the stent wire was completely degraded (Fig. 5A). H&E staining also revealed a similar BMAS degradation process. The stent wires showed irregular cracks (Fig. 5B), as well as a tendency to degrade from the circumference to the center, as revealed by SEM. The degradation process of the scaffold showed that the Mg content decreased gradually, while the Ca and P contents increased (Fig. 5C).

BMAS implantation did not induce any tissue damage

Next, we examined pathological changes in tissue sections of the heart, liver, spleen, lung, and kidney with H&E staining. We did not find any abnormal histological changes in the three groups (Fig. 6). Also, no significant differences in the blood indices were observed among the three groups during the follow-up period (Table 1). Thus, we concluded that the BMAS did not induce any pathological changes in any of the organs examined, at least during the first 4 months after stent implantation.

https://doi.org/10.3349/ymj.2019.60.5.429

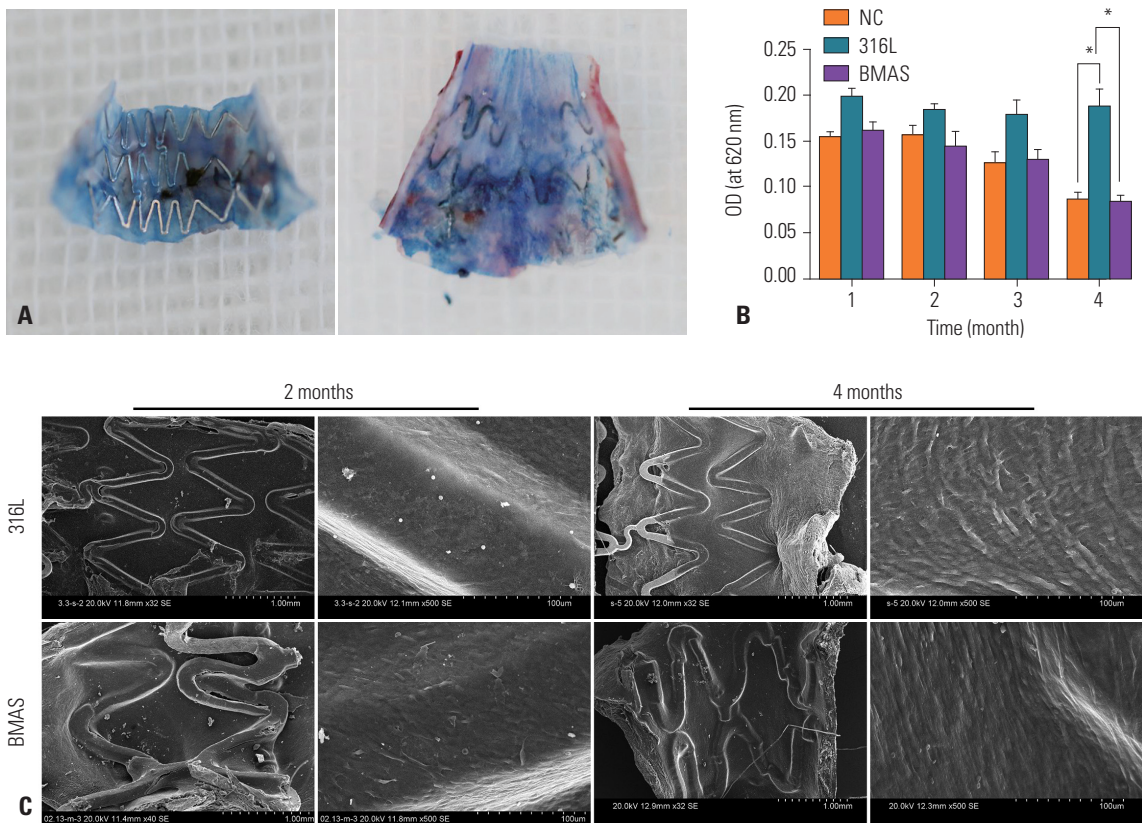

Fig. 4. Comparison of endothelial repair after stent implantation among the NC, 316L, and BMAS groups. (A) Evans blue staining was used to observe endothelial repair of the grafted vein. (B) Statistical analysis of endothelial repair among the three groups with absorbance at 620 nm. A high OD value means poor endothelial repair. (C) Examination of endothelial repair of the grafted vein by scanning electron microscopy. The surface of the BMAS was smoother than the 316L and the endothelium of the graft vein was better repaired. *p<0.05. NC, no-treatment control; 316L, 316L stainless steel stent; BMAS, biodegradable magnesium alloy stent.

DISCUSSION

The efficacy of using endovascular stent implantation for the treatment of VGF has been acknowledged. DESs have a better patency rate than BMSs, which are superior to balloon dilation.[11,12] Brennan, et al.[4] performed a comparative study on stents in 49325 older adult patients (age >65 years old) with SVG disease and found that, at the end of the 3-year follow-up period, DESs had a lower all-cause mortality rate than BMSs (22.7% vs. 28.0%, p<0.001; 0.83–0.91); however, no significant differences were observed with regard to myocardial infarction or TLR. In addition, Pokala, et al.[5] compared the effects of the first and second generation of DESs in SVG disease treatment and concluded that both the first- and second-generation DESs showed high event rates, but did not show any significant difference in all-cause mortality in patients with myocardial infarction or TLR, suggesting that the existing stents did not show a satisfactory therapeutic efficacy in the treatment of SVG. Therefore, it is imperative to devise new stents to reduce adverse outcomes of patients with SVG.

Vascular injury repair and remodeling are typically completed within 6–12 months, and thereafter, the permanent metal stent offers no benefit to the vessel. A biodegradable stent is an effective means with which to solve this problem in a number of ways. For instance, it can provide mechanical support in the early stage after the operation and can be absorbed by the body through degradation to restore the diastolic contractile function of vessels.[13,14] Previous animal experiments[8,15] and clinical findings[9,10,16] have suggested that BMASs are most likely to change the current treatment method due to their excellent characteristics. In the present study, we observed that the BMAS effectively supported VG anastomosis and increased the diameter of the lumen within 1–3 months after implantation. After BMAS implantation, morphological changes were induced within 2–3 months, and the radial force was gradually reduced. At the end of the 4-month observation, no obvious loss of the lumen diameter was observed. Therefore, we believe that a BMAS offers great benefits to a VG during the first 1–3 months, which is the critical period for injured vessels to regain function.

In-stent restenosis is the main cause of failure after stent implantation. The main pathological manifestation is excessive intimal proliferation.[17] The proliferation and migration of VSMCs plays an important role in this pathological process.[18] Sternberg, et al.[19] applied different concentrations of Mg^{2+} *in vitro* to explore its effects on VSMCs and vascular endothelial cells (VECs)

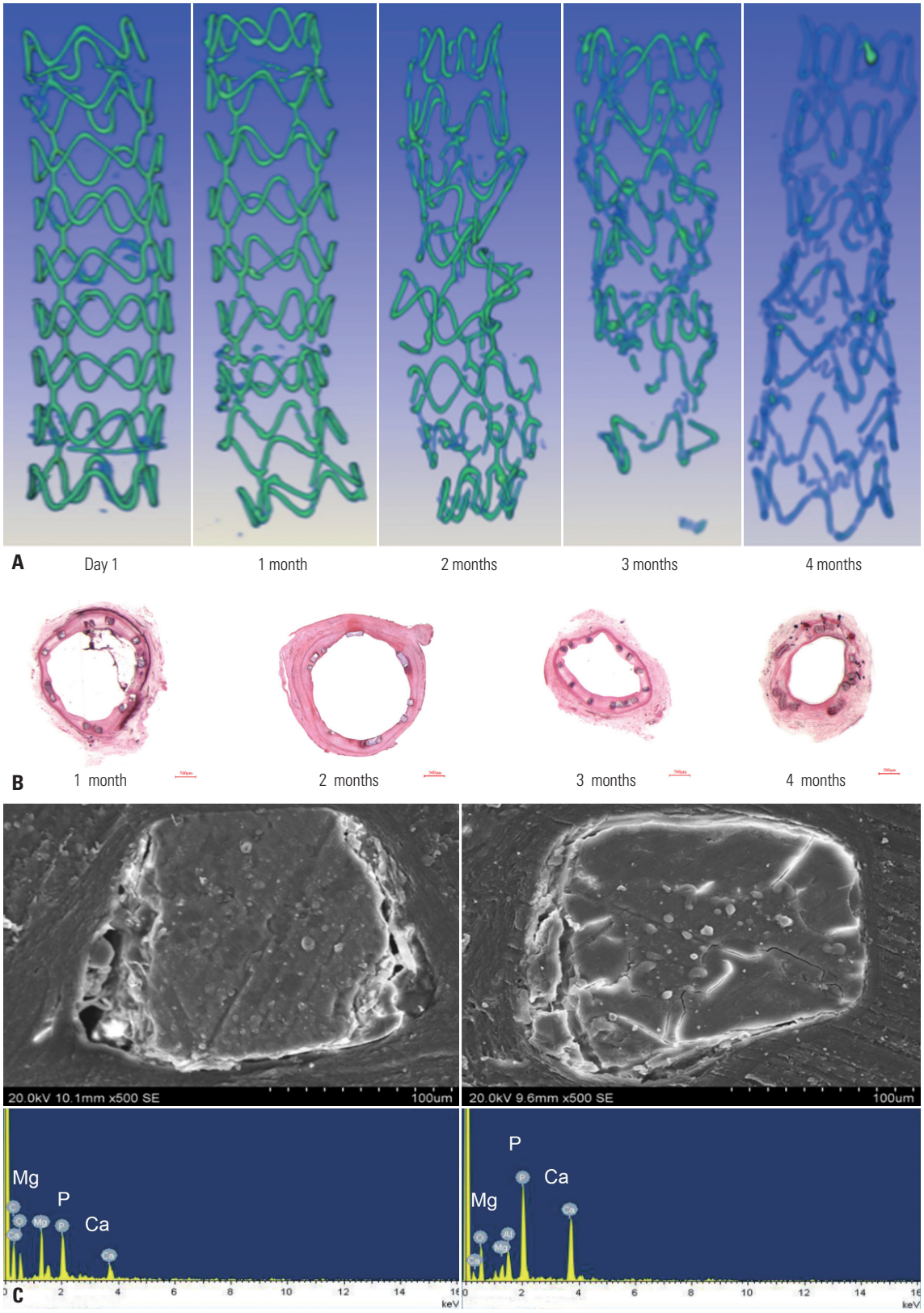

Fig. 5. Examination of the BMAS degradation process. (A) Stent morphology by X-ray tomography *in vitro*. The continuity of the stent was gradually lost, and the contrast of the bracket has changed, which means the metal content had changed. (B) Hematoxylin and eosin staining showing a BMAS tissue section (×63). (C) Analysis of BMAS degradation products. The analysis showed that the Mg content decreased gradually, while the Ca and P contents increased. BMAS, biodegradable magnesium alloy stent.

https://doi.org/10.3349/ymj.2019.60.5.429

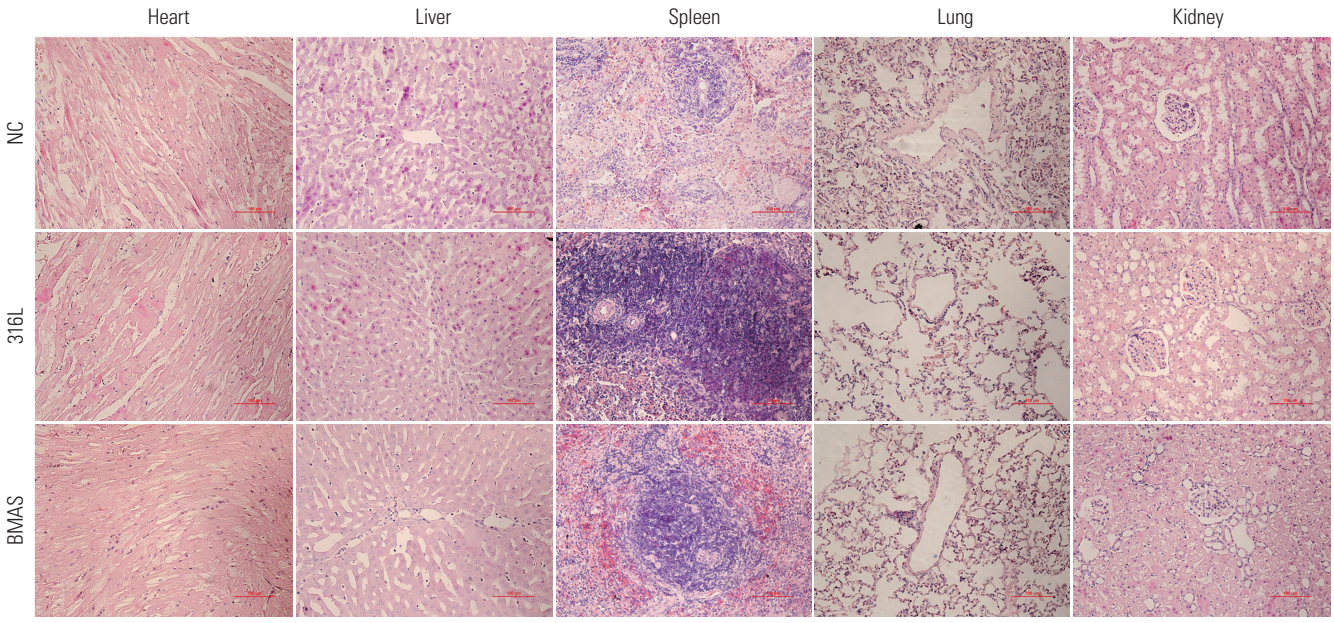

Fig. 6. BMAS implantation did not induce any tissue damage. Hematoxylin and eosin staining was performed on tissue sections prepared from different organs as indicated. Magnification, ×400. BMAS, biodegradable magnesium alloy stent.

Table 1. Comparison of Plasma Biochemical Indices of the Control, 316L, and BMAS Groups at 1 Month after Stent Implantation

	NC	316L	BMAS	*p* value
K (mmol/L)	3.47±0.67	3.30±0.40	3.09±0.38	0.428
Na (mmol/L)	136.28±5.08	135.47±9.60	137.27±3.89	0.901
Cl (mmol/L)	92.06±4.29	89.30±9.17	89.33±5.15	0.747
ALT (U/L)	61.40±16.92	56.00±19.18	52.17±19.09	0.719
ALKP (U/L)	82.40±24.91	62.00±26.40	57.33±20.53	0.233
TP (g/L)	53.38±5.96	51.28±9.09	57.12±4.83	0.362
ALB (g/L)	28.64±3.54	28.92±6.32	28.63±1.65	0.992
TBIL (μmol/L)	4.66±1.20	3.48±0.91	4.16±1.45	0.301
Urea (mmol/L)	5.54±0.91	7.18±1.59	5.73±2.07	0.214
CREA (μmol/L)	75.80±19.64	69.50±11.91	73.20±25.33	0.893
Ca (mmol/L)	3.20±0.25	3.20±0.28	3.18±0.15	0.976
P (mmol/L)	1.72±0.28	1.72±0.46	1.77±0.27	0.961
Mg (mmol/L)	1.13±0.26	1.03±0.14	0.92±10.11	0.162
FIB (g/L)	3.67±1.30	4.25±1.49	3.41±1.68	0.411

NC, no-treatment control; 316L, 316L stainless steel stent; BMAS, biodegradable magnesium alloy stent; ALT, alanine aminotransferase; ALKP, alkaline phosphatase; TP, total protein; ALB, human albumin; TBIL, total bilirubin; CREA, creatinine; FIB, fibrinogen.

and found that Mg^{2+} inhibited VSMC proliferation and promoted VEC proliferation. Moreover, Ma, et al.[20] reported that Mg^{2+} induced VMSC biphasic responses in a dose-dependent manner. A low concentration of Mg^{2+} was beneficial to the biological activity of VSMCs, while a high concentration was toxic. Furthermore, Waksman, et al.[15] implanted BMASs and stainless steel stents into the coronary arteries of pigs and observed that at the 28-day and 3-month time points, the intimal area of the BMAS was significantly smaller than that of a stainless steel stent. Additionally, Li, et al.[21] implanted a BMAS eluting with rapamycin (SEBMAS) into the lower abdominal aorta after balloon injury and found that the SEBMAS was able to further reduce neointimal proliferation. In the present study, we found that the neointimal area of the BMAS group was slightly larger than that of the NC and 316L groups at 2 months. This result may be due to a decrease in radial force, which resulted in neointimal proliferation. However, the area growth rate of the BMAS group was obviously lower than that of the 316L group at the later follow-up time point, indicating that the BMAS was more effective than 316L in reducing neointimal area growth.

Vascular re-endothelialization is an important process in vascular injury repair, and delay of endothelialization is the major cause of intimal hyperplasia and thrombosis. Although a number of studies have examined the effects of Mg on neo-

intimal formation, few studies have analyzed the impact of Mg on re-endothelialization. Maier, et al.[22] found that 10 mM $MgCl_2$ stimulated the proliferation of VECs. In addition, Zhao, et al.[23] showed that Mg has a concentration-dependent effect on the cellular biological activity and that a low concentration of $MgCl_2$ (<20 mM) promotes the migration of VECs. These findings together suggested that the BMAS has an advantage in promoting re-endothelialization. In line with these observations, we found that, compared to the 316L stent, the BMAS prompted re-endothelialization at an earlier time point after implantation, which is conducive to avoiding thrombosis and other adverse events. At present, animal studies and clinical trials have been performed on newly developed drug-eluting BMASs.[10,21] Our team has also designed a rapamycin-eluting BMAS, and the related tests are underway. While drug elution from a BMAS has a better effect on inhibiting neointimal proliferation, it also delays the process of re-endothelialization. Therefore, the gains and losses need to be carefully weighed before its clinical application.

The existing BMAS degradation time was usually within 2–12 months after implantation.[10,24] The stents used in the present study were treated with chemical conversion coating and polymer coating, and were degraded within 4 months after implantation. Mg was not observed by X-ray, which made the stents difficult to follow up for further examination using regular methods. This characteristic brought difficulties in the implantation and follow-up observation. It was difficult to observe the overall situation of the stent by adding platinum, tantalum, or other metal points as the marker. Our team successfully used color Doppler ultrasound to view the degradation process of BMASs *in vivo*. Compared to intravascular ultrasound and optical coherence tomography, this noninvasive method is more convenient and cost-efficient, and it is suitable for the clinical follow-up of implanted BMASs in the future. At the same time, we used XRT to evaluate BMAS degradation *in vitro* using different microstructure contrast imaging methods. Our findings suggested that XRT can be used to reveal the differences in the rate of degradation of different parts of the scaffold, thus providing the basis for improving the scaffold design.

Although BMAS exhibits many advantages over conventional stents, it also has its own disadvantages. For instance, Mg has a poor corrosion resistance, and a high concentration of Mg^{2+} (>50 mM) inhibits the migration of endothelial cells and reduces the adhesion between a cell and a substrate. Also, the quick metal degradation has been shown to decrease the local pH, which subsequently triggers inflammation and hemolysis.[25] In addition, whether elastic recoil and negative remodeling can occur during the stent degradation process has been an issue of concern.[26] Therefore, the rate of degradation of the BMAS needs to be tightly controlled so that the degradation products may offer benefits to vessel remodeling. In the present study, we treated the BMAS surface to reduce the rate of degradation, and we did not observe any severe inflammatory reaction. However, due to technical limitations, we were not able to follow the Mg^{2+} concentration or the local pH during degradation.

The present study had a number of limitations. First, the remodeling of the VG after complete degradation of the BMAS needs further examination. Second, how the degradation products of the BMAS are absorbed remains unknown. Third, the proposed mechanisms underpinning BMAS-mediated VG remodeling needs to be further corroborated in future studies.

In conclusion, we demonstrated in the present study that the BMAS is safe and efficient for the treatment of VG restenotic anastomosis, as evidenced by the following: 1) no thromboembolism was observed during the follow-up period; 2) the diameter loss and neointimal area of the anastomosis were smaller than those of the 316L stent, and re-endothelialization was better than with the 316L stent; and 3) no significant toxicity was observed. Therefore, our study provides a basis for the potential clinical application of the BMAS in VGF treatment in the future.

ACKNOWLEDGEMENTS

This research was funded by the National Natural Science Foundation of China (No. 81000136).

AUTHOR CONTRIBUTIONS

Conceptualization: Yugang Li. Data curation: Yugang Li, Lei Wang. Formal analysis: Lei Wang. Funding acquisition: Shijie Xin. Investigation: Dan Yu. Methodology: Yugang Li, Dan Yu. Project administration: Yugang Li, Lei Wang. Resources: Shanshan Chen. Software: Shanshan Chen. Supervision: Yugang Li, Lei Wang. Validation: Weifeng Sun. Visualization: Weifeng Sun. Writing—original draft: Yugang Li, Shijie Xin. Writing—review & editing: Yugang Li, Shijie Xin.

ORCID iDs

Yugang Li https://orcid.org/0000-0002-1155-6958
Lei Wang https://orcid.org/0000-0001-6582-5183
Shanshan Chen https://orcid.org/0000-0003-4561-0083
Dan Yu https://orcid.org/0000-0002-6824-447X
Weifeng Sun https://orcid.org/0000-0002-0107-0276
Shijie Xin https://orcid.org/0000-0001-6278-8794

REFERENCES

1. Mohr FW, Morice MC, Kappetein AP, Feldman TE, Ståhle E, Colombo A, et al. Coronary artery bypass graft surgery versus percutaneous coronary intervention in patients with three-vessel disease and left main coronary disease: 5-year follow-up of the randomised, clinical SYNTAX trial. Lancet 2013;381:629-38.
2. Habib RH, Dimitrova KR, Badour SA, Yammine MB, El-Hage-Sleiman AK, Hoffman DM, et al. CABG versus PCI: greater benefit in long-term outcomes with multiple arterial bypass grafting. J Am Coll Cardiol 2015;66:1417-27.
3. Harskamp RE, Lopes RD, Baisden CE, de Winter RJ, Alexander JH. Saphenous vein graft failure after coronary artery bypass surgery: pathophysiology, management, and future directions. Ann

https://doi.org/10.3349/ymj.2019.60.5.429

Surg 2013;257:824-33.
4. Brennan JM, Sketch MH Jr, Dai D, Trilesskaya M, Al-Hejily W, Rao SV, et al. Safety and clinical effectiveness of drug-eluting stents for saphenous vein graft intervention in older individuals: results from the medicare-linked National Cardiovascular Data Registry(®) CathPCI Registry(®) (2005-2009). Catheter Cardiovasc Interv 2016;87:43-9.
5. Pokala NR, Menon RV, Patel SM, Christopoulos G, Christakopoulos GE, Kotsia AP, et al. Long-term outcomes with first- vs. second-generation drug-eluting stents in saphenous vein graft lesions. Catheter Cardiovasc Interv 2016;87:34-40.
6. Stone GW, Rizvi A, Newman W, Mastali K, Wang JC, Caputo R, et al. Everolimus-eluting versus paclitaxel-eluting stents in coronary artery disease. N Engl J Med 2010;362:1663-74.
7. Kedhi E, Joesoef KS, McFadden E, Wassing J, van Mieghem C, Goedhart D, et al. Second-generation everolimus-eluting and paclitaxel-eluting stents in real-life practice (COMPARE): a randomised trial. Lancet 2010;375:201-9.
8. Heublein B, Rohde R, Kaese V, Niemeyer M, Hartung W, Haverich A. Biocorrosion of magnesium alloys: a new principle in cardiovascular implant technology? Heart 2003;89:651-6.
9. Haude M, Erbel R, Erne P, Verheye S, Degen H, Böse D, et al. Safety and performance of the drug-eluting absorbable metal scaffold (DREAMS) in patients with de-novo coronary lesions: 12 month results of the prospective, multicentre, first-in-man BIOSOLVE-I trial. Lancet 2013;381:836-44.
10. Haude M, Ince H, Abizaid A, Toelg R, Lemos PA, von Birgelen C, et al. Safety and performance of the second-generation drug-eluting absorbable metal scaffold in patients with de-novo coronary artery lesions (BIOSOLVE-II): 6 month results of a prospective, multicentre, non-randomised, first-in-man trial. Lancet 2016;387:31-9.
11. Levine GN, Bates ER, Blankenship JC, Bailey SR, Bittl JA, Cercek B, et al. 2011 ACCF/AHA/SCAI Guideline for Percutaneous Coronary Intervention. A report of the American College of Cardiology Foundation/American Heart Association Task Force on Practice Guidelines and the Society for Cardiovascular Angiography and Interventions. J Am Coll Cardiol 2011;58:e44-122.
12. Cutlip DE, Windecker S, Mehran R, Boam A, Cohen DJ, van Es GA, et al. Clinical end points in coronary stent trials: a case for standardized definitions. Circulation 2007;115:2344-51.
13. Peuster M, Beerbaum P, Bach FW, Hauser H. Are resorbable implants about to become a reality? Cardiol Young 2006;16:107-16.
14. Hermawan H, Dubé D, Mantovani D. Developments in metallic biodegradable stents. Acta Biomater 2010;6:1693-7.
15. Waksman R, Pakala R, Kuchulakanti PK, Baffour R, Hellinga D, Seabron R, et al. Safety and efficacy of bioabsorbable magnesium alloy stents in porcine coronary arteries. Catheter Cardiovasc Interv 2006;68:607-17.
16. Ghimire G, Spiro J, Kharbanda R, Roughton M, Barlis P, Mason M, et al. Initial evidence for the return of coronary vasoreactivity following the absorption of bioabsorbable magnesium alloy coronary stents. EuroIntervention 2009;4:481-4.
17. Curcio A, Torella D, Indolfi C. Mechanisms of smooth muscle cell proliferation and endothelial regeneration after vascular injury and stenting: approach to therapy. Circ J 2011;75:1287-96.
18. Farb A, Weber DK, Kolodgie FD, Burke AP, Virmani R. Morphological predictors of restenosis after coronary stenting in humans. Circulation 2002;105:2974-80.
19. Sternberg K, Gratz M, Koeck K, Mostertz J, Begunk R, Loebler M, et al. Magnesium used in bioabsorbable stents controls smooth muscle cell proliferation and stimulates endothelial cells in vitro. J Biomed Mater Res B Appl Biomater 2012;100:41-50.
20. Ma J, Zhao N, Zhu D. Biphasic responses of human vascular smooth muscle cells to magnesium ion. J Biomed Mater Res A 2016;104:347-56.
21. Li H, Zhong H, Xu K, Yang K, Liu J, Zhang B, et al. Enhanced efficacy of sirolimus-eluting bioabsorbable magnesium alloy stents in the prevention of restenosis. J Endovasc Ther 2011;18:407-15.
22. Maier JA, Bernardini D, Rayssiguier Y, Mazur A. High concentrations of magnesium modulate vascular endothelial cell behaviour in vitro. Biochim Biophys Acta 2004:1689:6-12.
23. Zhao N, Zhu D. Endothelial responses of magnesium and other alloying elements in magnesium-based stent materials. Metallomics 2015;7:118-28.
24. Slottow TL, Pakala R, Okabe T, Hellinga D, Lovec RJ, Tio FO, et al. Optical coherence tomography and intravascular ultrasound imaging of bioabsorbable magnesium stent degradation in porcine coronary arteries. Cardiovasc Revasc Med 2008;9:248-54.
25. Zhang E, Chen H, Shen F. Biocorrosion properties and blood and cell compatibility of pure iron as a biodegradable biomaterial. J Mater Sci Mater Med 2010;21:2151-63.
26. Maeng M, Jensen LO, Falk E, Andersen HR, Thuesen L. Negative vascular remodelling after implantation of bioabsorbable magnesium alloy stents in porcine coronary arteries: a randomised comparison with bare-metal and sirolimus-eluting stents. Heart 2009;95:241-6.